USDA Forest Service
Research Paper INT-69
1969

HEAT TRANSFER AND FIRE SPREAD

Hal E. Anderson

INTERMOUNTAIN FOREST AND RANGE EXPERIMENT STATION
Ogden, Utah 84401

USDA Forest Service
Research Paper INT-69
1969

HEAT TRANSFER AND FIRE SPREAD

Hal E. Anderson

Research partially supported by the Advanced Research Projects Agency, Department of Defense, under ARPA Order 818. This report has been cleared for open publication.

INTERMOUNTAIN FOREST AND RANGE EXPERIMENT STATION
Forest Service
U.S. Department of Agriculture
Ogden, Utah 84401
Joseph F. Pechanec, Director

THE AUTHOR

HAL E. ANDERSON has been Project Leader of the Fuel Science Research Work Unit since 1966. He joined the staff of Intermountain Station's Northern Forest Fire Laboratory at Missoula, Montana, in 1961 and served as Project Leader of the Fire Physics Project from 1962 to 1966. Prior to employment with the Forest Service he was with the General Electric Company and worked on thermal and nuclear instrumentation from 1952 to 1961. His B.S. degree in physics was obtained at Central Washington State College in 1952.

CONTENTS

GENERAL PROBLEM

Research in fire physics and fuel science at the Northern Forest Fire Laboratory (Missoula, Montana) is directed toward understanding and describing fire propagation through forest fuels and determining how the rate of fire spread is influenced by atmospheric, topographic, and fuel variables. Considerable qualitative information has been collected over the years; but quantitative data have become available only recently. An increase in this information has raised new questions and posed new problems. One fundamental question is: What are the relative roles of the several mechanisms of heat transfer (radiation, convection, conduction, and mass transport) in activating and sustaining the spread of fire?

Test fires in mat-type fuel beds of pine needles burned in still air and with controlled wind conditions demonstrated that radiation significantly influenced fire spread in still air (Rothermel and Anderson 1966). Several mathematical models of fire spread by the various heat transfer mechanisms have been developed and tested to some degree (Fons 1946; Emmons 1963; Hottel et al. 1965; Thomas and Law 1965). From this research and from results of our own experiments, we have developed and tested a mathematical description of fire spread (under no-wind condition) based on radiant heat transfer. This paper presents the development of the mathematical description, and the test procedures and results, and compares data from these tests with those from other fire research.

DEVELOPMENT OF MATHEMATICAL DESCRIPTION

MOISTURE CONTENT

Fuel moisture content has long been recognized as a major influence on ignition and fire spread (Gisborne 1928); therefore, any mathematical description of fire spread must include the influence of moisture. My approach to this task is to estimate the total heat required to remove the moisture and subsequently raise the fuel to ignition temperature. Various earlier researchers (Fons 1950; Martin 1964; Simms 1960, 1961, 1963) indicate a temperature of 300° to 380°C. typifies the pilot ignition point. Research at the Northern Forest Fire Laboratory (Mutch 1964) showed that a temperature of 320°C. (608°F.) would produce pilot ignitions in ground forest fuels. This temperature agrees with results of other research and was selected to represent pilot ignition temperature.

The energy required to remove the water contained in a pound of wet fuel and then to ignite it was determined from data published by Byram et al. (1952). These data were developed into an equation that estimates the energy input per pound of fuel at any moisture content up to 20 percent of ovendry weight. The equation takes into account the heat required to raise the fuel to ignition, the heat required to raise the moisture to boiling temperature, the heat of desorption, the latent heat of vaporization, and the variation in boiling temperature with moisture content. Until now, no consideration had been given to the endothermic heat of pyrolysis that leads to the ignition of fuel.

$$Q_{ig} = C_F(T_i - T_1) + C_w\Big[M(T_2 - T_1) + \Big[71\Big(\frac{M^{0.83}}{0.83}\Big)\Big]_o^M - M(71M^{-0.169})\Big] + L_t\Big[\Big(\frac{T}{71}\Big)^{-5.92}\Big]_{T_1}^{T_2} + H(M)_{T_1} \qquad (1)$$

where:

Q_{ig} = B.t.u./lb. (cal./g.)

C_F = 0.327, specific heat of fuel

C_w = 1.0, specific heat of water

T_1 = ambient temperature

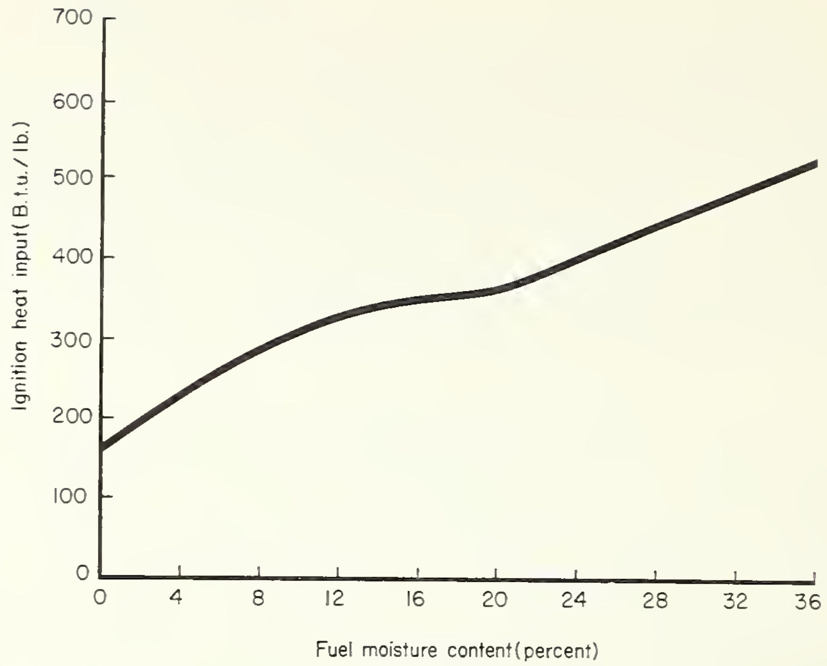

Figure 1.--Heat required to bring 1 pound of fuel to ignition as a function of fuel moisture content.

T_2 = boiling temperature

T_i = ignition temperature 608°F. (320°C.)

L_t = latent heat of vaporization

M = moisture content, lb./lb. (g./g.)

$H(M)T_1$ = heat of desorption (16 cal./g.).

Using this equation, we developed a curve (figure 1) to show the relation of energy input to moisture content of the fuel (in percent).

Additional definitions are listed in the Appendix.

RADIANT HEAT

We knew how much heat was required to raise the moist fuel to ignition and the temperature at ignition. Our next step was to develop an equation that would describe the change in rate of spread. Research by Thomas (1963) and Emmons (1963) indicated that the heat flux from the fire to unburned fuel can be related to rate of spread. Assuming that the energy required to cause ignition remains constant and that the emissive power of the fire remains constant--just high enough to cause ignition when the fire reaches the unburned fuel--we can write:

$$Q = \int_0^\infty E\, e^{-ax} dt \qquad (2)$$

where:

Q = heat per vertical cross section of the fuel bed to cause ignition, B.t.u./ft.^{2}
E = emissive power of the fire, B.t.u./ft.^{2} - hr.$^{-}$
a = attenuation constant
x = distance from the fire front to the fuel particle or elemental volume in question, ft.
t = time, hr.

This can be modified by:

$$dt = \frac{dx}{R}$$

where:

R = steady rate of spread, ft./hr.

Substituting and integrating equation (2):

$$R = \frac{E}{aQ} \tag{3}$$

The quantity, Q = B.t.u./ft.^{2}, must be modified so Q_{ig}, B.t.u./lb. can be used. This is accomplished by:

$$Q = \frac{Q_{ig}\rho_f}{\sigma_a/4} \tag{4}$$

where:

ρ_f = fuel particle density, lb./ft.^{3} (g./cm.^{3})

$\sigma_a/4$ = fuel particle projected surface area to volume ratio, ft.^{2}/ft.^{3} (cm.^{2}/cm.^{3}).

The attenuation factor "a" must be put into some measurable form. It is assumed to be proportional to the total projected area of fuel in a unit volume of space (Committee on Fire Research, 1961, p. 126).

$$a = \frac{1}{4\lambda} \tag{5}$$

where:

λ = void volume per total surface area

1/4 = projected portion of surface area.

Equations 4 and 5 are substituted in equation 3, which takes the form:

$$R = \frac{\sigma_a \lambda E}{\rho_f Q_{ig}} \tag{6}$$

This mathematical description states that the rate of spread is dependent on the emissive power of the fire and will be modified by the size of the fuel particles, σ_a; porosity of the fuel bed, λ; density of the fuel particles, ρ_f; and the amount of energy required for ignition (primarily a function of the amount of moisture in the fuel), Q_{ig}. The emissive power of the fire is made up of two components: (1) the combustion zone within the fuel bed; (2) the flame plume above the fuel bed. Both components contribute to radiant heating. However, convective heating takes place only in the fuel bed and in the region of the fuel bed-fire plume interface. In the study reported herein we are concerned with describing rate of spread in absence of wind with the assumption that radiation was the primary source of heat.

The fuel descriptors are independent of the two source components. However, the contributions of heat to the fuel are dependent on the relative weight and influence of each mode of heat transfer. The radiant heat from each component is defined thus:

$E_c = \sigma \varepsilon_c T_c^4$ (combustion zone emissive power)

$E_f = \sigma \varepsilon_f T_f^4$ (flame emissive power).

The impact of the flame's emissive power on the fuel ahead of the fire is a function of distance and shape of the flame; these must be taken into account. This modification describes the irradiance of the element. By integrating the configuration factor, F_{12}, over the distance of influence and dividing by the configuration factor for an infinite plane source integrated over 1 foot for the two components transferring radiant heat, a numerical value, F_{12}', is obtained; it describes the magnitude of the heat impact of each component. The absorptivity of the fuel element is considered equal to unity; however, the radiant heat loss of the element to its surroundings is regarded as negligible.

Equation 6 was modified to show these considerations:

$$R = \frac{\sigma_a \lambda}{\rho_f Q_{ig}} [\sigma \varepsilon_c T_c^4 \quad F_{12}' \quad + \sigma \varepsilon_f T_f^4 \quad F_{12}'] \tag{7}$$

An earlier report (Anderson 1968) showed that the variation in flame irradiance can be important. The configuration factor for the combustion zone was determined prior to testing. However, the flame configuration factor had to be determined later from photographs of the flame shape. A form of equation 7 was tested against data collected from earlier testing (Anderson and Rothermel 1965) and was found to agree with rates of spread previously observed. We designed a study program to investigate unknowns in equation 7 and to determine whether radiant heat could account for rate of spread under the no-wind condition.

CONVECTIVE HEAT

We recognized that radiant heat might not account for all the heat; so we had to determine a convective heat transfer coefficient for the needles. For this, some measure of the gas velocity in the fuel bed had to be derived. Also, the Reynolds and Nusselt numbers were essential for calculating the convective heat transfer coefficient h_c. The research previously reviewed by Hottel (Blinov and Khudiakov 1959) and presented by Thomas (1963) showed two expressions for Reynolds number:

$$N_{RE} = \frac{V_L d}{\nu} \tag{8}$$

$$N_{RE} = \frac{m_1}{\mu d} \tag{9}$$

where:

V_L = regression rate of liquid burning surface

d = characteristic dimension, pan diameter or flame depth

ν = kinematic viscosity = μ/ρ_g

μ = dynamic viscosity

ρ_g = gas density

m_1 = rate of weight loss.

Equation 9 can be put into the same form as equation 8 by rearranging terms:

$m_1 = \rho_b A V_F$, lb./sec.

$A = d^2$

$\mu = \nu \rho_g$

V_F = linear regression rate of fuel surface, ft./sec.

ρ_b = bulk density of fuel bed

$$N_{RE} = \frac{m_1}{\mu d} = \frac{\rho_b d^2 V_F}{\nu \rho_g d} = \frac{V_F d}{\nu} \left(\frac{\rho_b}{\rho_g}\right). \tag{10}$$

The quantity $V_F\left(\frac{\rho_b}{\rho_g}\right)$ represents the gas velocity, V_g, at the surface of the fuel, and V_F is the same as the V_L used by Hottel. Multiplying the regression rate of the surface by the ratio of fuel density to gas density provides the value of the gas velocity at the surface. This means that liquid-pool fires and solid-fuel fires should correlate.

BULK DENSITY OF FUEL BED

We noted a similarity between equation 6 and the equation published by Thomas and Law (1965). The equations are equivalent in concept except that $\sigma_a\lambda/\rho_f$ is replaced by $1/\rho_b$ (bulk density of the fuel bed). These two quantities are approximately equal; the exact relation can be determined by considering the properties of the fuel particle and fuel bed. The porosity of a fuel bed, λ, is defined as:

$$\lambda = \frac{V_1 - V_2}{\sigma_a V_2} \tag{11}$$

where: λ = porosity, ft.^{3}/ft.^{2}

σ_a = fuel particle surface area-to-volume ratio, ft.^{2}/ft.^{3}

V_1 = fuel bed volume, ft.^{3}

V_2 = fuel particles volume, ft.^{3}

Rearranging this equation we have:

$$\sigma_a\lambda + 1 = V_1/V_2 \tag{12}$$

The volumes of the fuel bed, V_1, and the fuel particles, V_2, are proportional to the respective densities:

$V_1 = W_b/\rho_b$ and $V_2 = W_b/\rho_f$

where W_b is the weight of the fuel. Combining these terms and substituting into equation 12, the result is:

$$\sigma_a\lambda + 1 = \rho_f/\rho_b \quad \text{or} \quad 1/\rho_b = \frac{\sigma_a\lambda}{\rho_f} + \frac{1}{\rho_f}. \tag{13}$$

This relation exists for fuel beds made up of a single size of fuel. In more complex fuel beds, the bulk density provides a gross estimate; whereas appraising by size classes, variation of particle density, and proportion of each size class provides a more accurate estimate. For the present, we are considering only homogeneous beds of a single fuel.

FLAME AND BURNING CHARACTERISTICS

Information that would enable us to predict flame size or burning rates from a given fuel complex is not yet available; hence, it is difficult to estimate rates of fire spread accurately. Factors that affect flame size and burning rate include: (1) physical properties of the fuel bed and of the fuel particles; and (2) chemical properties of the fuel elements (e.g., crude fat content, silica-free ash content, and the amount of cellulose and/or hemicellulose in the fuel. Investigations are being conducted at the Northern Forest Fire Laboratory to determine how much the chemical properties of the fuel influence flammability--discussion of such investigations is outside the scope of this paper.

The physical properties of fuels are also under study at the Laboratory and include fuel particle size, thermal properties, fuel bed porosity and continuity, and several other factors. These are of importance to the spread equation since some enter the fuel descriptor set, $\sigma\lambda/\rho_f Q_{ig}$. Frequently it has been observed that the residence time of flame at a given point in a fuel bed is related to diameter of the fuel particle. A review of fire research literature and unpublished tests here at the Laboratory indicate that residence time is a function of particle diameter (Fons et al. 1962; Byram et al. 1966; McCarter and Broido 1965; Wooliscroft and Law 1967).

TEST PROCEDURES

The measurements necessary to evaluate the rate of spread according to equation 7 were determined from the unknowns in the equation. These are the emissivities of the combustion and flame zones, the temperature of each zone, and the flame shape mean configuration factor for each zone. By comparing the calculated rate of spread to the observed rate we obtain a means of determining the relative importance of the role of radiant heat transfer in the propagation of fire. This does not give us any information about the generation of radiant energy. However, we gain some insight into the generation phase through measurements of weight loss, flame residence time, and radiant heat fluxes to the fuel.

Many of the methods mentioned above except for two have been described in previous publications (Anderson and Rothermel 1965; Anderson 1968). Two measurements not used in previous work are: determination of the configuration factor; and the radiant heat flux passing through a fuel element. Configuration factor determinations were made using the techniques described in "Flame Shape and Fire Spread" (Anderson 1968). A sequence of at least 10 photographs (1 second exposure at f:11 on Plus X film) in an overlay was used to determine average flame shape and length.

Radiant heat fluxes from the flame and the combustion zone were measured with Gardon-type heat rate sensors. These sensors were water cooled and shielded with sapphire windows so that only radiant heat was measured. The recorded millivolt signal from these sensors was corrected for transmissivity, percent radiation below the wavelength cutoff of the window, configuration factor, and view area enclosed. Besides indicating the heat flux passing through a particular point, the resulting values could be compared with the combustion and flame zone temperature measurements for calculation of the emissivity of each zone.

The heat rate sensors in the fuel bed were placed with the sensing element 0.5 inch below the surface of the fuel bed. Each sensor faced the oncoming fire front and was positioned to view all of the fire in the fuel bed. Thermocouples were located at the surface of the fuel bed and 0.5 inch below it to provide data on temperatures as the fire front approached and passed. The peak values represented the fire front's arrival and were used to calculate the blackbody emissive power of the combustion zone's fire front. The emissivity of the zone was determined by dividing the heat rate sensor value of heat flux by the calculated blackbody value.

The heat flux of the flame was measured in nearly the same manner as were the heat rate sensors in the fuel bed except the sensors were positioned so that one edge of their view angle coincided with the surface of the fuel bed. The sensor then viewed the space above the bed. Thermocouples, 5 mil chromel/alumel, were placed 2, 11, and

22 inches above the fuel bed surface to measure flame temperature. Analysis of the flame size for each test set (consisting of 3 or more fires) indicated which thermocouples were in the flame envelope. From these thermocouples an average flame temperature was determined. This was used to determine an average blackbody emissive power. The average emissive power of the flame was also determined by considering the heat rate sensor value at discrete distances from the flame. The emissivity of the flame was determined as described for the combustion zone.

A preliminary series of tests was made with ponderosa pine needle beds to assess the magnitude of the influence of porosity. Fuel beds of 0.5 and 1.0 ft.^{2} load area and constant loadings were burned as stationary fires with surface ignition. The fuel depth was varied to provide various porosities and measurements of weight loss and flame length were made.

The radiant heat fire tests were conducted with three replications in three pine needle fuels--ponderosa pine (Pinus ponderosa Laws.); western white pine (Pinus monticola Dougl.); and lodgepole pine (Pinus contorta Dougl.). The fuels were conditioned to moisture contents varying from 2.5 to 23 percent of ovendry weight. Ambient conditions were maintained at 90° F. with relative humidities of 7 to 92 percent; ambient conditions were matched to fuel moisture contents. Fuel beds were prepared according to established technique (Schuette 1965). A summary of the test conditions and fuel characteristics is given in table 1.

Table 1.--Ambient conditions and fuel characteristics for each test set

(A set constitutes three or more fires)

Fuel type & moisture content	Air temperature	Relative humidity	σ_a	Particle density ρ_f	λ	Heat to ignition Q_{ig}	Fuel heat content H
%	°F.	% RH	ft.^{2}/ft.^{3}	lb./ft.^{3}	ft.^{3}/ft.^{2}	B.t.u./lb.	B.t.u./lb.
PP - 2.6	90.5	7.0	1,741	31.8	9.1×10^{-3}	213	8,744
PP - 4.2	90.5	13.2	1,741	31.8	8.8×10^{-3}	237	8,744
PP - 5.3	90.5	22.2	1,741	31.8	9.1×10^{-3}	254	8,744
PP - 5.9	90.7	30.7	1,741	31.8	8.5×10^{-3}	262	8,744
PP - 8.6	90.8	51.5	1,741	31.8	8.5×10^{-3}	300	8,744
PP - 14.0	90.3	75.3	1,741	31.8	8.5×10^{-3}	347	8,744
PP - 20.5	90.5	92.2	1,741	31.8	8.4×10^{-3}	377	8,744
WP - 3.4	90.6	6.1	2,790	33.5	5.9×10^{-3}	227	8,457
WP - 6.7	91.1	21.6	2,790	33.5	5.6×10^{-3}	275	8,457
WP - 7.4	90.5	30.9	2,790	33.5	5.5×10^{-3}	283	8,457
WP - 10.1	90.8	51.2	2,790	33.5	5.6×10^{-3}	317	8,457
WP - 15.3	90.4	75.8	2,790	33.5	5.6×10^{-3}	353	8,457
WP - 21.6	90.5	91.3	2,790	33.5	5.6×10^{-3}	388	8,457
LPP - 3.6	92.2	6.2	2,188	35.4	4.6×10^{-3}	230	8,748
LPP - 5.4	90.8	21.9	2,188	35.4	4.8×10^{-3}	260	8,748
LPP - 6.5	90.8	31.0	2,188	35.4	4.3×10^{-3}	270	8,748
LPP - 8.8	90.8	51.1	2,188	35.4	4.5×10^{-3}	301	8,748
LPP - 13.4	90.7	75.8	2,188	35.4	4.9×10^{-3}	345	8,748
LPP - 23.2	90.1	91.0	2,188	35.4	5.0×10^{-3}	402	8,748

PP is ponderosa pine
WP is western white pine
LPP is lodgepole pine

TEST RESULTS AND DISCUSSION

ROLE OF FUEL DESCRIPTORS

During the development of the equation to describe fire spread in terms of radiant heat transfer, a group of fuel descriptors was established. This group, $\sigma_a\lambda/\rho_f Q_{ig}$, can be determined prior to a test fire; by correlating it to the rate of spread, a best estimate of the heat flux can be obtained. Figure 2 shows the results of 3 or more test fires averaged at each condition. Taking an increment along the linear portion of the curve, the maximum heat flux into the fuel is found to be 40 X 10^3 B.t.u./ft.^{2} - hr. (3.0 cal./cm.^{2} - sec.). Low fuel moisture contents resulted in the high rates of spread and as moisture content increased a point was reached where a departure from a linear relation occurred. Following the departure to zero rate of spread, the intercept represents the point where moisture content prevents fire spread. By determining Q_{ig} and referring to figure 1, the moisture contents for no spread were found:

Ponderosa pine: $\sigma_a\lambda/\rho_f Q_{ig} = 1.13 \text{ X } 10^{-3}$, $Q_{ig} = 412 \frac{\text{B.t.u.}}{\text{lb.}}$

MC = 24.2 percent

Western white pine: $\sigma_a\lambda/\rho_f Q_{ig} = 1.13 \text{ X } 10^{-3}$, $Q_{ig} = 412 \frac{\text{B.t.u.}}{\text{lb.}}$

MC = 24.2 percent

Lodgepole pine: $\sigma_a\lambda/\rho_f Q_{ig} = 0.81 \text{ X } 10^{-3}$, $Q_{ig} = 359 \frac{\text{B.t.u.}}{\text{lb.}}$

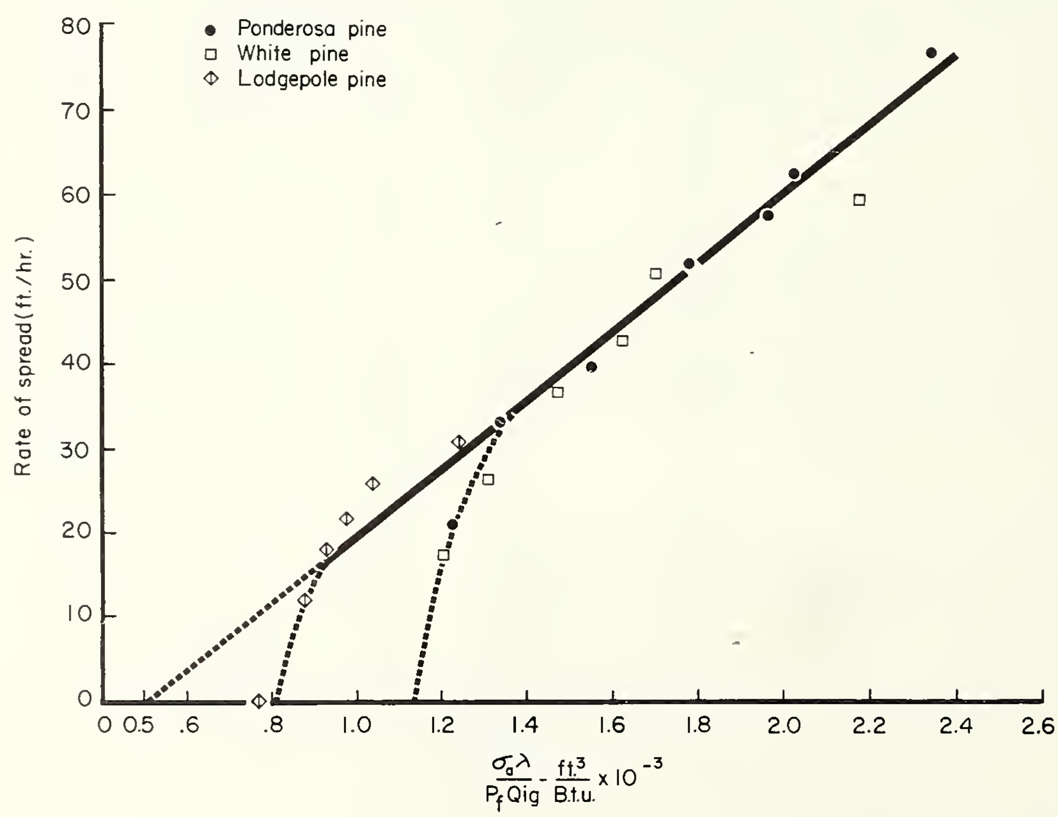

Figure 2.--A near linear relation is exhibited between the experimental rate of spread and the fuel descriptor's set. Note the rolloff at the low end.

Table 2.--Calculated maximum heat fluxes associated with rate of spread and the fuel descriptors

Fuel type & moisture content	$\frac{\sigma_a \lambda}{\rho_f Q_{ig}}$	Experimental rate of spread R_E	Heat flux $q_{T/A}$	
%	ft.^{3}/B.t.u.	ft./hr.	B.t.u./ft.^{2} - hr.	Cal./cm.^{2} - sec.
PP - 2.6	2.34×10^{-3}	76.1	3.26×10^4	2.46
PP - 4.2	2.02×10^{-3}	61.8	3.06×10^4	2.30
PP - 5.3	1.96×10^{-3}	57.0	2.90×10^4	2.18
PP - 5.9	1.78×10^{-3}	51.6	2.90×10^4	2.18
PP - 8.6	1.55×10^{-3}	39.6	2.56×10^4	1.93
PP - 14.0	1.34×10^{-3}	33.0	2.46×10^4	1.85
PP - 20.5	1.22×10^{-3}	21.0	1.74×10^4	1.31
WP - 3.4	2.17×10^{-3}	58.8	2.71×10^4	2.04
WP - 6.7	1.70×10^{-3}	50.4	2.96×10^4	2.23
WP - 7.4	1.62×10^{-3}	42.6	2.63×10^4	1.98
WP - 10.1	1.47×10^{-3}	36.6	2.49×10^4	1.88
WP - 15.3	1.32×10^{-3}	26.4	2.00×10^4	1.51
WP - 21.6	1.20×10^{-3}	17.4	1.45×10^4	1.09
LPP - 3.6	1.24×10^{-3}	30.6	2.47×10^4	1.86
LPP - 5.4	1.14×10^{-3}	25.8	2.26×10^4	1.70
LPP - 6.5	$.98 \times 10^{-3}$	21.6	2.21×10^4	1.66
LPP - 8.8	$.93 \times 10^{-3}$	18.0	1.94×10^4	1.46
LPP - 13.4	$.88 \times 10^{-3}$	12.0	1.36×10^4	1.02
LPP - 23.2	$.77 \times 10^{-3}$			

PP is ponderosa pine
WP is western white pine
LPP is lodgepole pine

The values for ponderosa and western white pine are in agreement with previous laboratory findings. Fires in lodgepole pine needle beds at 23.2 percent MC would not spread even with repeated ignition of the fuel bed leading edge substantiating the above cutoff value. The porosity of this fuel appears to be the factor responsible but additional work with variations in porosity is needed to substantiate this.

RADIANT HEAT

The total heat flux related to fire spread was calculated for each set of test fires. These values are tabulated in table 2. The radiant heat fluxes reported by Thomas and Law (1965) are of the same magnitude where σ and/or λ were varied. This general agreement indicates radiant heat does contribute to rate of spread, but in the present case the energy is the combined sum of the heat transfer components. The next step was to determine how much heat was being supplied by the flame and how much by the combustion zone. Analysis of all the tests showed a nearly constant combustion zone temperature with no significant correlation to fuel moisture content.

Table 3.--Test results for each fuel type and moisture condition

(Values are average of three or more fires in each set.)

Fuel type & moisture content	R	t_R	D	L	B	T_c	T_f	ε_f	$\int F_{12}$	$\int F_{12}$	E_f*
%	ft./hr.	min.	ft.	ft.	lb./min.	°F.	°F.		Flame	Comb. zone	B.t.u./ft.- hr.
PP - 2.6	76.1	1.27	1.61	5.5	0.98	1591	1680	0.28	1.18	0.08	6.22×10^3
PP - 4.2	61.8	1.27	1.31	5.0	.77	1591	1627	.28	1.19	.08	9.46×10^3
PP - 5.3	57.0	1.27	1.20	4.7	.81	1591	1570	.28	1.11	.08	8.70×10^3
PP - 5.9	51.6	1.27	1.09	4.3	.70	1591	1509	.28	1.07	.08	8.88×10^3
PP - 8.6	39.6	1.27	.84	3.5	.57	1591	1507	.28	.95	.08	6.58×10^3
PP - 14.0	33.0	1.27	.70	2.9	.35	1591	1392	.28	.85	.08	6.33×10^3
PP - 20.5	21.0	1.27	.44	2.0	.17	1591	1254	.28	.71	.08	1.97×10^3
WP - 3.4	58.8	.92	.90	2.2	.35	1434	1321	.16	.60	.08	4.03×10^3
WP - 6.7	50.4	.92	.78	2.0	.31	1434	1380	.16	.58	.08	3.31×10^3
WP - 7.4	42.6	.92	.65	1.9	.31	1434	1531	.16	.57	.08	4.28×10^3
WP - 10.2	36.6	.92	.56	1.5	.27	1434	1450	.16	.46	.08	3.64×10^3
WP - 15.3	26.4	.92	.40	1.1	.26	1434	1311	.16	.40	.08	2.88×10^3
WP - 21.6	17.4	.92	.27	.9	.20	1434	1229	.16	.35	.08	1.73×10^3
LPP- 3.6	30.6	1.06	.54	1.5	.21	1492	1548	.16	.43	.08	3.20×10^3
LPP- 5.4	25.8	1.06	.46	1.5	.19	1492	1548	.16	.42	.08	4.50×10^3
LPP- 6.5	21.6	1.06	.38	1.1	.13	1492	1303	.16	.36	.08	4.7×10^3
LPP- 8.8	18.0	1.06	.32	.9	.14	1492	1358	.16	.33	.08	3.9×10^3
LPP- 13.4	12.0	1.06	.21	.7	.12	1492	1135	.16	.20	.08	

*Average of heat flux sensor signal.

PP is ponderosa pine
WP is western white pine
LPP is lodgepole pine

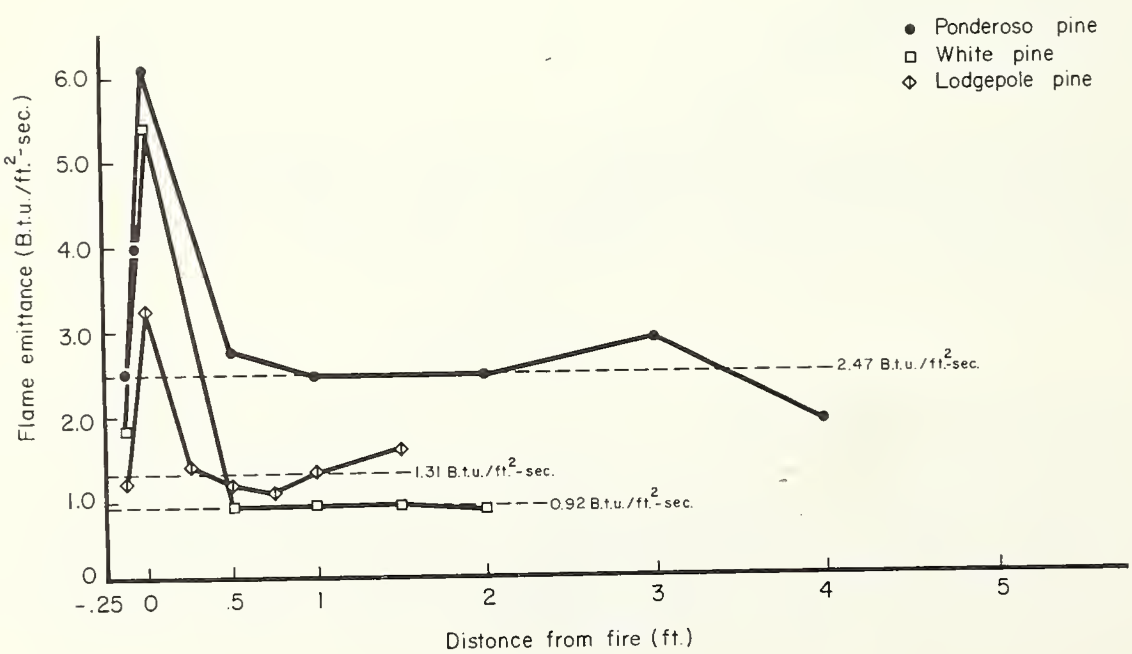

Figure 3.--Flame emittance calculations from heat rate sensors for fires in fuel beds at 6-percent moisture content.

The different fuel types produced a slight difference in the average temperature of the combustion zone, as follows:

Fuel type	Average temperature
Ponderosa pine	1591° F. (867° C.)
Western white pine	1434° F. (779° C.)
Lodgepole pine	1492° F. (811° C.)

These combustion zone temperatures are not unusual if moisture is removed from the fuel before the fire front or combustion zone reaches it. The irradiance of the fuel could change with moisture content changes because emissivity varied or the absorptivity of the intervening gases varied. The heat rate sensors for the combustion zone were placed too close to the surface of the fuel and were not sufficiently collimated. As a result, poor repeatability was obtained. However, these measurements did indicate a rather constant heat flux from the combustion zone. We found no decrease in heat flux with increases in fuel moisture content; this tended to support the thermocouple data but due to the lack of repeatability no reliable estimate of combustion zone emissivity could be made. The equation was evaluated for rate of spread by using a value of 1.0 for the combustion zone.

The thermocouples located above the fuel bed showed that the average flame temperature decreased as fuel moisture content increased:

Fuel type	Temperature range (°F.)	Rate of change (°F./percent MC)
Ponderosa pine	1680 - 1254	24
Western white pine	1531 - 1229	24
Lodgepole pine	1548 - 1135	42

Also, the burning rate, flame length, and flame depth were found to decrease in this same manner,as shown in table 3. These three parameters along with flame temperature govern the emissive power of the flame. The values obtained from the heat rate sensors do show a decrease with moisture increase but not as rapidly as the above variables of burning rate, flame length and depth. The emissive power values derived from the heat rate sensors at various distances from the flame agreed very closely with the values determined after the sensors had entered the flame (figure 3). The average emissive power was obtained from these values and compared with the blackbody emissive power determined by the thermocouple readings to calculate the emissivity of each test set (figure 4). Ponderosa pine fuel beds produced taller and thicker flames than the other fuels which generated flames with smaller dimensions; the calculated emissivities are substantiated by these physical characteristics of the flames.

By using the data of the emissive powers we can estimate the total radiant heat flux that has an impact on the fuel ahead of the fire. The values of heat flux can be calculated according to equation 7 and summed for comparison with the total heat flux found to be necessary to produce the measured rate of spread (see table 2). The results of this analysis are shown in figure 5 with the summed radiant heat flux as a percentage of the total heat flux and plotted against fuel moisture content. The radiant heat fluxes were determined by using a combustion zone emissivity of 1.00 and flame emissivities of 0.28 for ponderosa pine fires and 0.16 for lodgepole and western white pine fires.

This analysis shows that radiant heat can account for 40 percent or less of the total heat flux necessary for the fire spread observed in these fuel beds. The rest of the heat flux must come from some other heat transfer mechanism. Conduction appears to be insignificant; a brief analysis indicated only 1/50 of the necessary energy would be available through this mechanism. This means convective heat transfer must be the primary source through some horizontal transport mechanism.

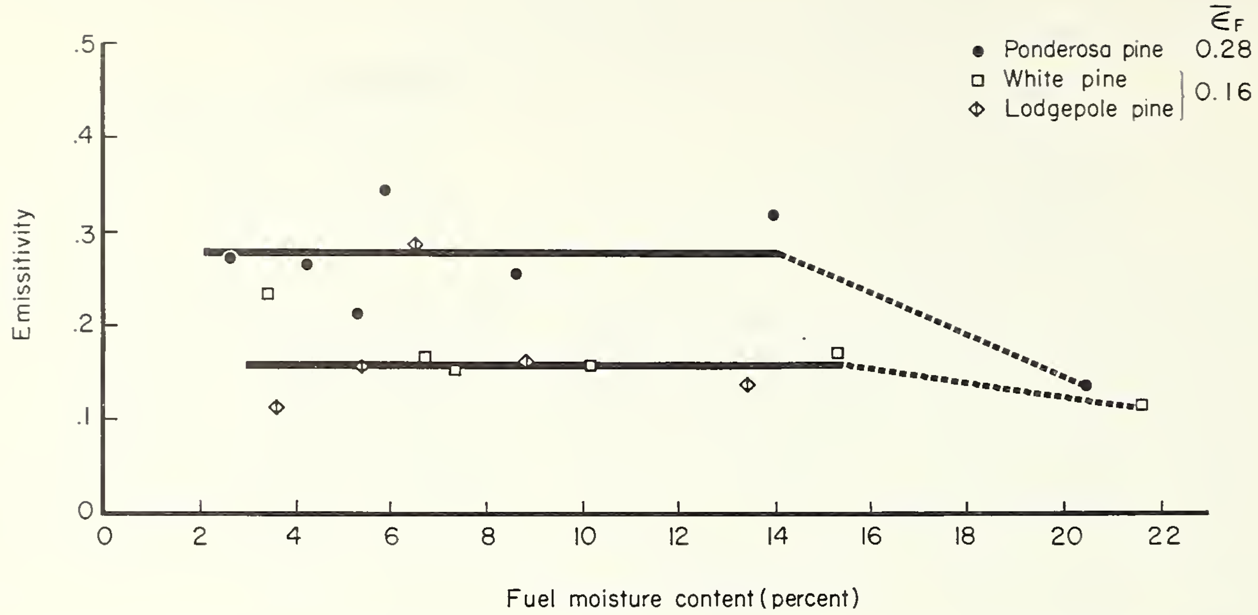

Figure 4.--Flame emissivities for fires in three fuels at the same environmental conditions were determined from heat flux sensor measurements.

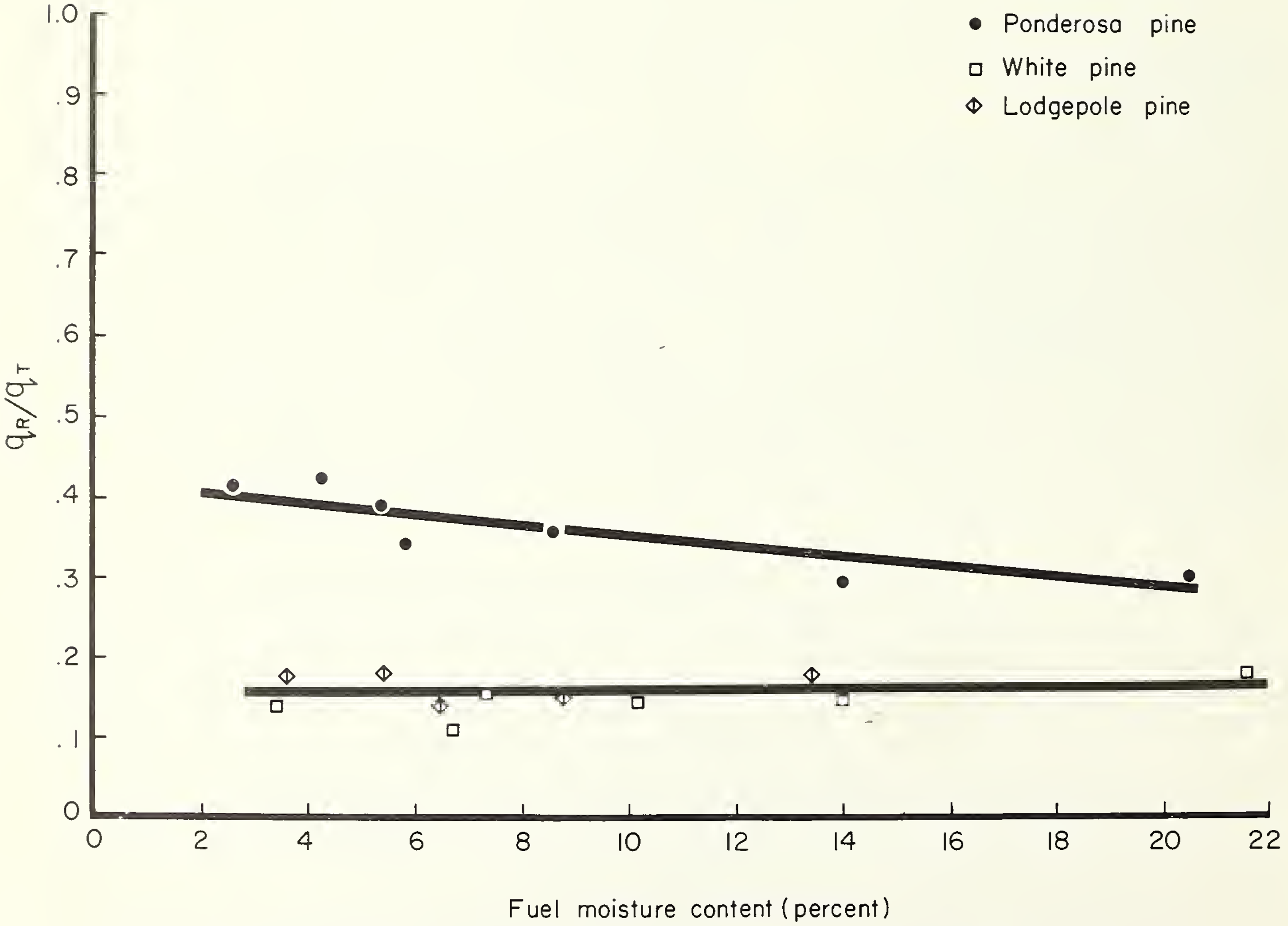

Figure 5.--Portion of total heat flux contributable to radiant heat flux.

CONVECTIVE HEAT

As mentioned earlier, it was necessary to determine a convective heat transfer coefficient. In addition, both the Reynolds and the Nusselt numbers had to be computed. Using the procedures outlined previously, a gas velocity and Reynolds number were calculated for each test set. If solid fuel fires respond in a manner similar to liquid pool fires, then nearly equal values of Reynolds numbers should occur for fires of similar dimensions. Figure 6 shows how the solid fuel fires grouped near the curve for gasoline pool fires. The same forces seem to apply to the various fires resulting in turbulent, transitional, and laminar regimes. Fires in ponderosa pine beds with less than 9 percent moisture content were turbulent and in the transitional regime for moisture contents above 9 percent. All fires in western white pine and lodgepole pine were in the transitional or laminar regimes.

Values for the gas velocity in each test set were determined and were used with the diameter of the fuel particle to determine the Reynolds number. The Nusselt number for cylinders was used to calculate the convective heat transfer coefficient. This combined with the temperature difference between the combustion zone and the ambient air provided a measure of the convective heat transfer component.

In all tests the calculated convective heat flux exceeded the net heat flux which is obtained by subtracting the radiant heat flux from the total heat flux values in table 2. This means that a horizontal transfer efficiency coefficient does exist. This horizontal transfer coefficient was calculated for each fuel:

Ponderosa pine: $\eta = (0.90 - 0.014\ MC^*)$
Western white pine: $\eta = (1.00 - 0.028\ MC)$
Lodgepole pine: $\eta = (1.00 - 0.036\ MC)$

---

*MC is the fuel moisture content in percent.

These coefficients infer less heat transfer in ponderosa fuel of low moisture contents and a more rapid decrease in heat transfer for western white pine and lodgepole pine fuels because their burning regimes are transitional or laminar.

Incorporating the horizontal transfer coefficients into equation 7 the new description of fire spread by heat transfer becomes:

$$R = \frac{\sigma\ \lambda}{\rho_f Q_{ig}} \left[\sigma\varepsilon_c T_c^4 \left(\int_0^\infty F_{12}dx\right) + \sigma\varepsilon_F T_F^4 \left(\int_0^\infty F_{12}dx\right) + \eta h_c (T_c - T_1)\right] \tag{14}$$

where:

T_c = combustion zone temperature

T_1 = ambient air temperature.

Values for each component of the equation were obtained for the experimental data. The resulting rates of spread are compared to the experimental values in figure 7. The equation was found to describe rate of spread quite accurately but does point out the following areas where additional research is needed:

1. Estimation prior to a fire of how much flame will be generated.

2. Is there a physical limitation to fire spread caused by maximum heat flux into the fuel bed?

3. What is the relation between fuel bed characteristics and convective heat transfer?

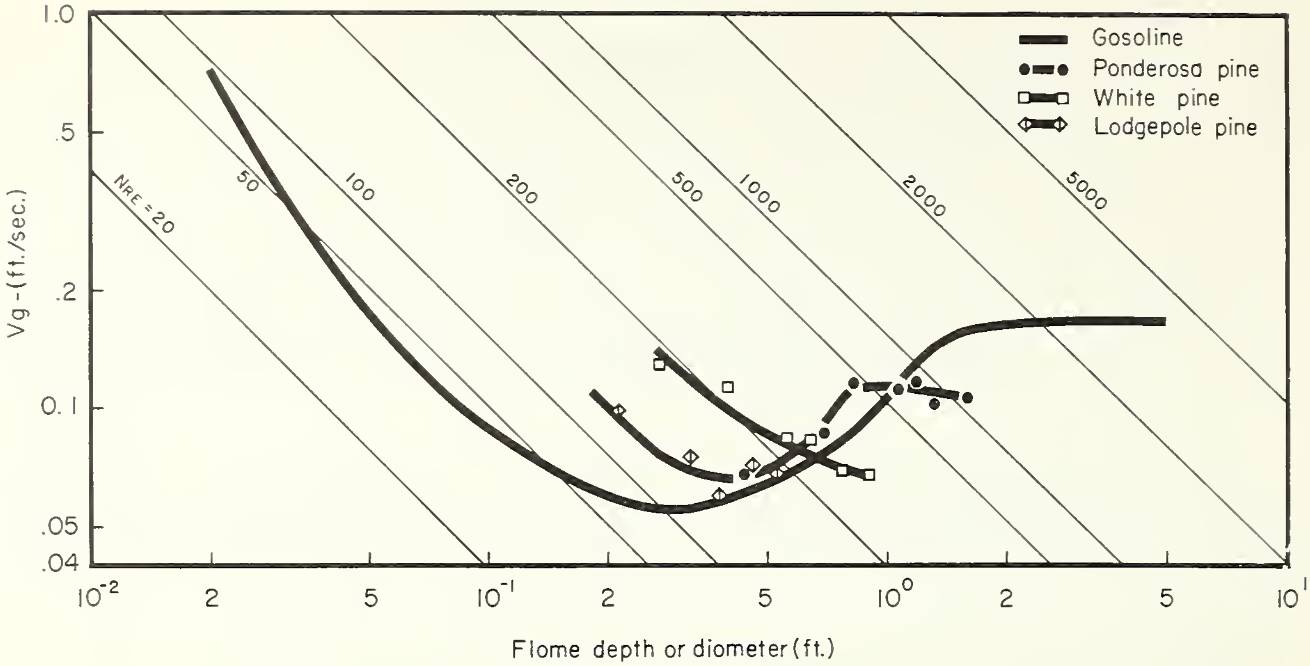

Figure 6.--Burning regimes of various fuels based on cold vapor density and viscosity.

Figure 7.--Comparison of experimental rates of spread to theoretical curve of fire spread showing end points for fuel moisture content.

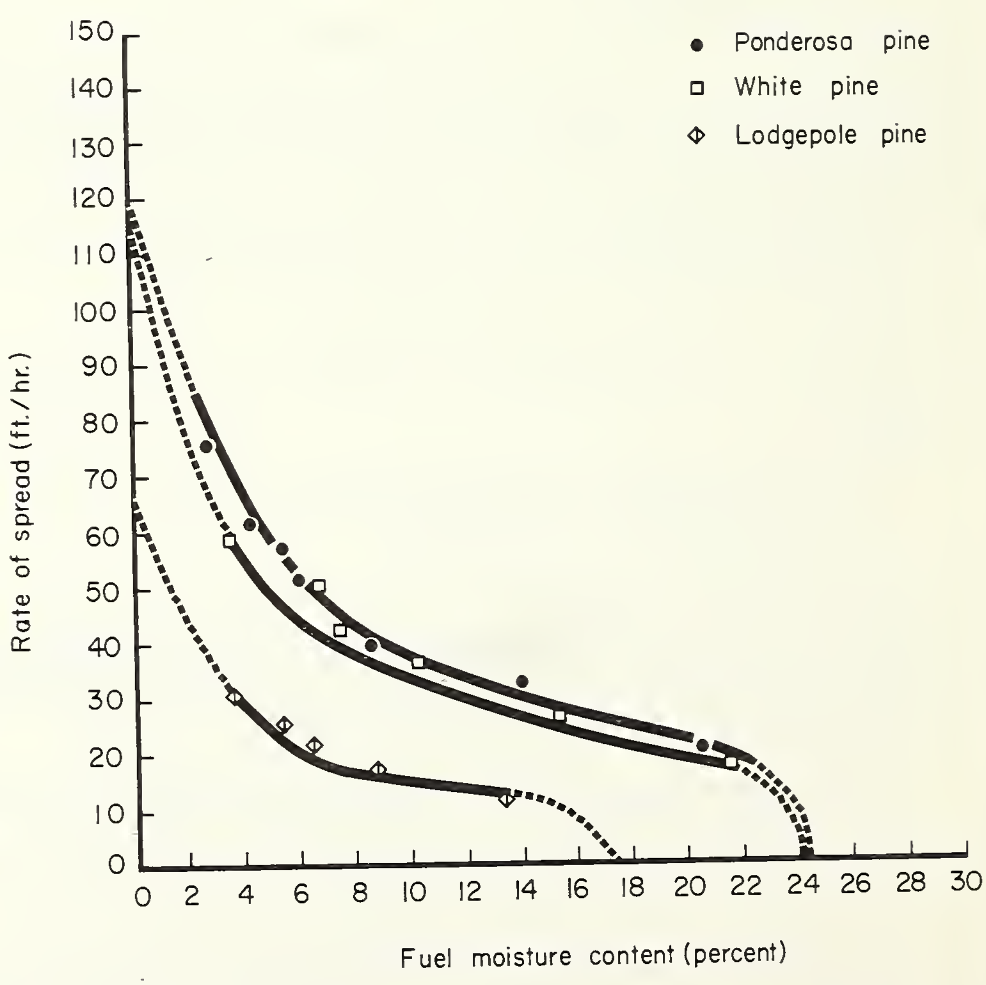

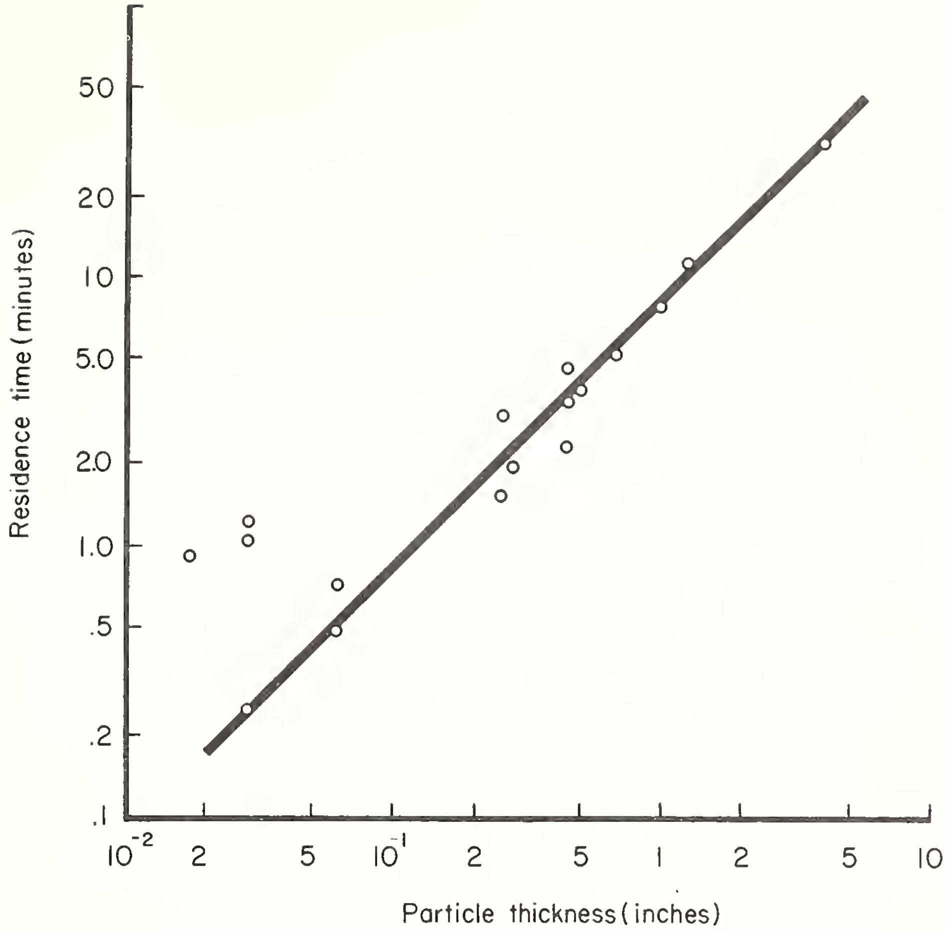

Figure 8.--Relation of residence time to particle thickness determined from measurements made during test fires.

4. Over what range of particle sizes and bed porosities does the fuel descriptor set apply?

Values for the combustion zone and flame temperatures determined experimentally were used to test equation 14 against fires in beds of different widths. This was done for the fires described in "Fire Spread and Flame Shape" (Anderson 1968). The equation yielded a rate of spread that was within: 99 percent of the experimental rate of spread for a 1.5-foot-wide ponderosa pine bed; 77 percent to 89 percent for 5.0-foot beds; 103 percent for a 1.5-foot-wide bed of western white pine; and 89 percent for 5.0-foot-wide beds. Rate of spread was overestimated at 136 percent of the experimental value for 5-foot-wide beds of lodgepole pine primarily because the flame depth measurements differed by a factor of three. In addition, the flame-shielded test (Rothermel and Anderson 1966) was used and the value from the equation was 97 percent of the experimental spread assuming no radiant heat from the flame. These evaluations support the credibility of the equation and further work will determine whether this approach is applicable to a variety of fuels.

FIRE RESPONSE TO σ AND λ

In fuel beds where the particles are loosely arranged, each particle will burn in a manner predominantly controlled by its own thermal properties. The energy feedback to the particle from surrounding fuel elements and their pyrolysis products will influence the burning characteristics but may be a nearly constant value until the particles are very far apart or very close together. This idea was checked by plotting research data for a variety of particle sizes ranging from 1.75×10^{-2} to 4.00 inches against the residence time or duration of active flaming. The results shown in figure 8 suggest that in porous fuel beds, residence time in minutes is equal to 8 times the particle diameter or thickness in inches. At the low end of the curve the residence time for a single needle falls on the line. Those points above the line are residence times for the test fuel beds and have porosities from 4.3 to 9.1 X 10^{-3} ft.^{3}/ft.^{2}. Much of the other data were for fuel beds with porosities between 2.45 and 6.04 X 10^{-2} ft.^{3}/ft.^{2}. It would appear porosity has an important influence on the residence time and the burning rate of a fuel bed and rather small changes can make major changes in a fuel bed's burning characteristics.

The tests of stationary fires in fuel beds of fixed area and loading revealed the influence of porosity on burning rate and flame length. It was found that an optimum porosity exists where the fuel burning rate is maximum (figure 9). This occurs with loading held constant but as loading is increased, the maximum burning rate occurs at a different porosity. It is possible that as loading increases the burning rate will reach a nearly constant level over a large range of porosities. Additional work is in progress to fully evaluate porosity, area of combustion, and loading. The values of $\sigma_a\lambda$ for the three fuel types used in the main test series ranged from 10 for lodgepole to 18.9 for western white pine with ponderosa pine at 16. These values are on the low side of optimum porosity and any variation will have a significant effect on the fire's behavior. Comparing these results to porosities measured in the field, we found even lower porosities for the needle layer under a pure stand of ponderosa pine. Any disturbance to the forest floor litter layer increasing the spacing between needles can cause an increase in burning rate and more flaming activity. It appears the dimensionless group $\sigma_a\lambda$, may be a good indicator of potential fire spread in a fuel.

The influence of fuel particle density seems quite straightforward and follows the results presented by Fons et al. (1962). He shows that as the specific gravity of the fuel decreases the rate of spread increases. The location of ρ_f in the denominator of equation 14 reflects this behavior.

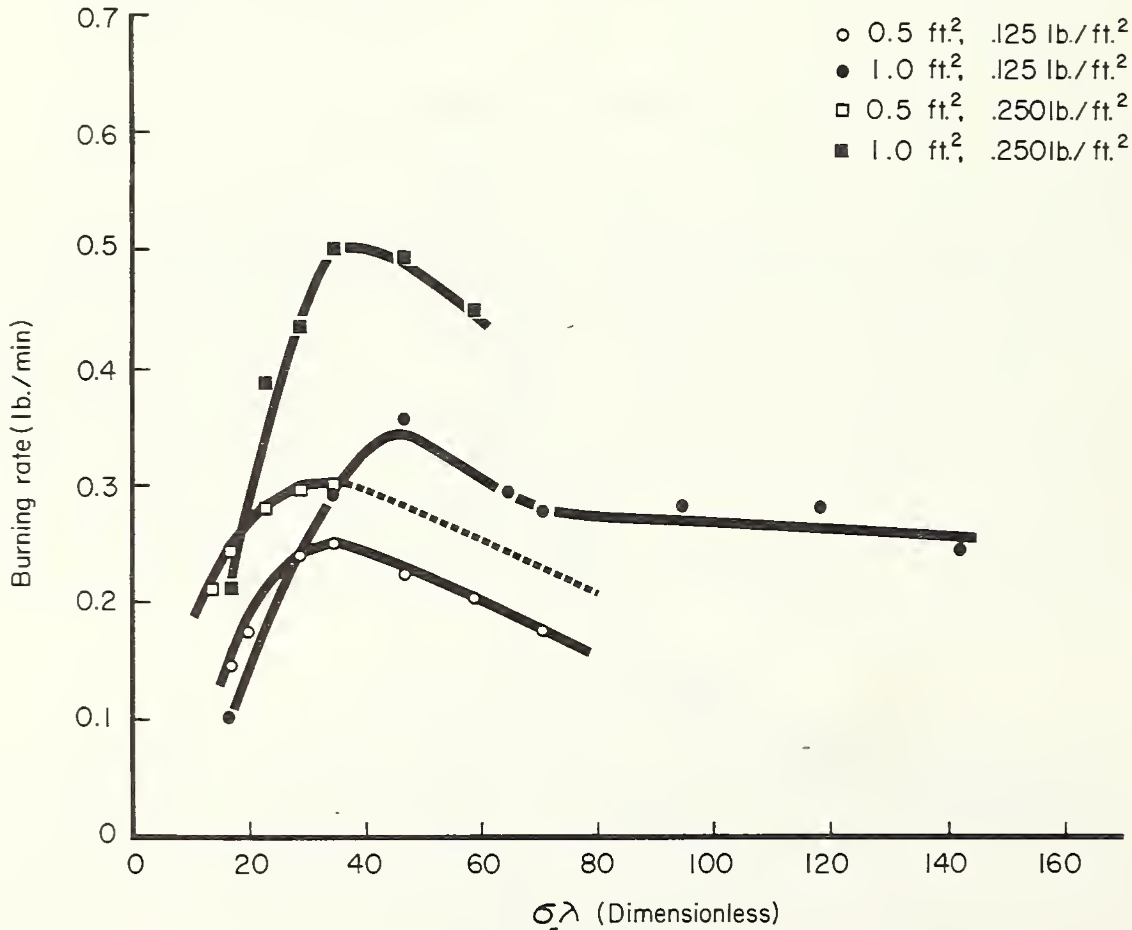

Figure 9.--Influence of porosity, λ, on burning rate for fires in ponderosa pine needles with a σ_a of 1,740 ft.^{2}/ft.^{3}. Each data point is average of three fires.

CONCLUSIONS

The work conducted to date indicates that radiant heat transfer can account for only 40 percent of the total heat flux necessary to sustain a spreading fire. Convective heat transfer at the interface of the combustion zone and the new fuel probably accounts for the rest. Burning characteristics and flame depth are strongly controlled by the fuel particle size and the porosity of the bed. In porous beds the residence time of a fire is controlled by the particle size. A direct relationship seems to exist between residence time and particle size.

Fuel beds of solid fuel elements can be correlated to liquid pool fires by using the ratio of fuel bed density to cold vapor gas density. Three burning regimes, turbulent, transitional, and laminar, exist in solid fuels and may contribute to discrepancies found among various sets of experimental fires.

A group of selected fuel descriptors consolidates the more important parameters into a measure of the bulk heat requirement, B.t.u./ft.^{3}, and, with the experimental rates of spread, indicates the maximum heat flux is near 40 X 10^3 B.t.u./ft.^{2} - hr. (3 cal./cm.^{2} - sec.).

The tallest flames and highest burning rates occur where an optimum porosity exists. Natural litter fuel beds appear to have low porosities and small changes can cause large shifts in burning rate.

LITERATURE CITED

Anderson, Hal E.
1968. Flame shape and fire spread. Fire Technol. 1968 (Feb.): 51-58, illus.

_______ and R. C. Rothermel.
1965. Influence of moisture and wind upon the characteristics of free-burning fires. Tenth Symp. (Int.) on Combust., pp. 1009-10-19, illus. Pittsburgh: The Combustion Institute.

Blinov, V. I., and G. N. Khudiakov.
1959. Certain laws governing diffusive burning of liquids. Reviewed by H. C. Hottel. Fire Res. Abstr. and Rev. 1(2): 41-44.

Byram, G. M., H. B. Clements, M. E. Bishop, and R. M. Nelson, Jr.
1966. An experimental study of model fires. Project Fire Model final report. U.S. Forest Serv., Southeastern Forest Exp. Sta., 51 pp., illus.

_______, F. M. Sauer, W. L. Fons, and R. K. Arnold.
1952. Thermal properties of forest fuels. U.S. Forest Serv., Fire Research, 34 pp., illus.

Committee on Fire Research.
1961. A study of fire problems. Nat. Acad. Sci., Nat. Res. Counc. Pub. 949, 174 pp., illus.

Emmons, Howard.
1963. Fire in the forest. Fire Res. Abstr. and Rev. 5(3): 163-178, illus.

Fons, Wallace L.
1946. Analysis of fire spread in light forest fuels. J. Agr. Res. 72: 93-121, illus.

Fons, Wallace L.
1950. Heating and ignition of small wood cylinders. Ind. and Eng. Chem. 42(10): 2130-2133, illus.

_______, H. B. Clements, E. R. Elliott, and P. M. George.
1962. Project Fire Model summary progress report II. U.S. Forest Serv., Southeastern Forest Exp. Sta., 55 pp., illus.

Gisborne, H. T.
1928. Measuring forest fire danger in northern Idaho. U.S. Dep. Agr. Misc. Pub. 29, 64 pp., illus.

Hottel, H. C., C. G. Williams, and F. R. Steward.
1965. The modeling of fire spread through a fuel bed. Tenth Symp. (Int.) on Combust., pp. 997-1007, illus. Pittsburgh: The Combustion Institute.

Martin, S.
1964. Ignition of organic materials by radiation. Fire Res. Abstr. and Rev. 6(2): 85-98, illus.

McCarter, R. J., and A. Broido.
1965. Radiative and convective energy from wood crib fires. Pyrodynamics 2: 65-85, illus.

Mutch, R. W.
1964. Ignition delay of ponderosa pine needles and sphagnum moss. J. Appl. Chem. 14: 271-275.

Rothermel, Richard C., and Hal E. Anderson.
1966. Fire spread characteristics determined in the laboratory. U.S. Forest Serv. Res. Pap. INT-30, 34 pp., illus.

Schuette, Robert D.
1965. Preparing reproducible pine needle fuel beds. U.S. Forest Serv. Res. Note INT-36, 7 pp., illus.

Simms, D. L.
1960. Ignition of cellulosic materials by radiation. Combust. and Flame 4(4): 293-300, illus.

_______.
1961. Experiments on the ignition of cellulosic materials by thermal radiation. Combust. and Flame 5(4): 369-375, illus.

_______.
1963. On the pilot ignition of wood by radiation. Combust. and Flame 7(3): 253-261, illus.

Thomas, P. H.
1963. The size of flames from natural fires. Ninth Symp. (Int.) on Combust., pp. 844-859. New York: Academic Press, Inc.

_______ and Margaret Law.
1965. Experiments on the spread of fire. Rep. on Forest Res. 1965: 124-130, illus.

Wooliscroft, M. J., and Margaret Law.
1967. A report on forest fire fieldwork. Joint Fire Res. Organ., Fire Res. Note 647, 14 pp., illus.

APPENDIX

Symbol	Definition	Measure
A	= area	ft.^{2}
C_f	= specific heat of fuel	0.327
C_w	= specific heat of water	1.000
D	= flame depth	ft.
E	= emissive power of fire	B.t.u./ft.^{2} - hr.
E_c	= combustion zone emissive power	B.t.u./ft.^{2} - hr.
E_f	= flame emissive power	B.t.u./ft.^{2} - hr.
F_{12}	= configuration factor	--
H	= fuel heat content	B.t.u./lb.
$H(M)_{T_1}$	= heat of desorption	B.t.u./lb.
L	= flame length	ft.
L_t	= latent heat of vaporization	B.t.u.
M	= moisture content	lb./lb.
MC	= fuel moisture content, ovendry	percent
N_{RE}	= Reynolds number	--
Q	= heat per vertical cross section of bed	B.t.u./ft.^{2}
Q_{ig}	= heat to raise 1 lb. fuel to ignition	B.t.u./lb.
R	= rate of spread	ft./hr.
T_1	= ambient temperature	°F.
T_2	= boiling temperature	°F.
T_F	= temperature of flame zone	°R
T_I	= ignition temperature	608°F.(320°C.)
T_c	= temperature of combustion zone	°R
V_1	= void volume per unit of load area	ft.^{3}/ft.^{2}
V_2	= fuel volume per unit of load area	ft.^{3}/ft.^{2}
V_F	= fuel bed regression burning rate	ft./sec.
V_L	= liquid burning velocity	ft./sec.

Symbol	Definition	Measure
a	= attenuation constant	ft.$^{-1}$
d	= characteristic dimension	ft.
h_c	= convective heat transfer coefficient	B.t.u./ft.^{2} - hr. - °
m	= weight loss rate	lb./sec.
$q_{T/A}$	= total heat flux	B.t.u./ft. - hr.
t	= time	hr.
t_b	= fuel bed depth	ft.
w_b	= weight of fuel per unit of load area	lb./ft.^{2}
x	= separation distance	ft.
ε_c	= emissivity of combustion zone	--
ε_f	= emissivity of flame zone	--
η	= horizontal convective heat transfer coefficient	--
λ	= bed void volume-to-surface area ratio	ft.^{3}/ft.^{2}
μ	= dynamic viscosity	--
ν	= kinematic viscosity	ft.^{2}/sec.
ρ_b	= bulk density of fuel bed	lb./ft.^{3}
ρ_f	= fuel particle density	lb./ft.^{3}
ρ_g	= gas density	lb./ft.^{3}
σ_a	= particle surface area-to-volume ratio	ft.^{2}/ft.^{3}
σ	= Stefan-Boltzman constant	B.t.u./ft. - hr. - °

Headquarters for the Intermountain Forest and Range Experiment Station are in Ogden, Utah. Field Research Work Units are maintained in:

- Boise, Idaho
- Bozeman, Montana (in cooperation with Montana State University)
- Logan, Utah (in cooperation with Utah State University)
- Missoula, Montana (in cooperation with University of Montana)
- Moscow, Idaho (in cooperation with the University of Idaho)
- Provo, Utah (in cooperation with Brigham Young University)

FOREST SERVICE CREED

The Forest Service of the U. S. Department of Agriculture is dedicated to the principle of multiple use management of the Nation's forest resources for sustained yields of wood, water, forage, wildlife, and recreation. Through forestry research, cooperation with the States and private forest owners, and management of the National Forests and National Grasslands, it strives — as directed by Congress — to provide increasingly greater service to a growing nation.